6 Reliability Analysis

6.1 Introductory Remarks

A very natural application of SFEM and the other probabilistic analytical and numerical methods [313] is the reliability assessment for both homogeneous [45,256,354] and heterogeneous structures [87,102,231,262]. The starting point of the analysis is to assume the limit state function in terms of any structural state parameters – displacements, stresses, temperatures or strains (as well as some combination of them in the coupled problems). Then, starting from statistical input on the structural parameter, probabilistic structural analysis is carried out and, finally, starting from the limit state function, the reliability index is computed. The reliability index should have the same properties as the classical Kolmogoroff probability and, in the same time, the damage function.

Following the stochastic structural analyses, First Order Reliability Method (FORM) and Second Order Reliability Method (SORM) are most frequently used [87,114,115,209]. The methods do not provide satisfactory results for non-symmetric PDF of the input and output in the same time and that is why the higher order moments are proposed. Considering numerous applications of the Weibull PDF in the composite material area, the corresponding Second Order Third Moment (W–SOTM) approach proposed for homogeneous media is described below. To illustrate this approach, let us denote the limit state function as g. The expected values, variances and skewnesses of this function are calculated or computed first using up to the second orders of this function, the limit state function derivatives with respect to the input random variables vector b as well as using its probabilistic moments (σ_i as a standard deviation). There holds

$$E[g] = g + \tfrac{1}{2}\sum_{i=1}^{n}\left(\frac{\partial^2 g}{\partial b_i^2}\right)\sigma_i^2 \tag{6.1}$$

$$\sigma^2(g) = \{g\}^2 + \sum_{i=1}^{n}\left[\left(\frac{\partial g}{\partial b_i}\right)^2 + g\frac{\partial^2 g}{\partial b_i^2}\right]\sigma_i^2 + \sum_{i=1}^{n}\left[\frac{\partial g}{\partial b_i}\frac{\partial^2 g}{\partial b_i^2}\right]S_i\sigma_i^2 - E^2[g] \tag{6.2}$$

$$S(g)=\left\{\{g\}^3+\tfrac{3}{2}\sum_{i=1}^{n}\left[2g\left(\frac{\partial g}{\partial b_i}\right)^2+g^2\frac{\partial^2 g}{\partial b_i^2}\right]\sigma_i^2\right. \tag{6.3}$$
$$\left.+\sum_{i=1}^{n}\left[\left(\frac{\partial g}{\partial b_i}\right)^3+3g\frac{\partial g}{\partial b_i}\frac{\partial^2 g}{\partial b_i^2}\right]S_i\sigma_i^3-E^3[g]-3E[g]\sigma(g)\right\}\frac{1}{\sigma^3(g)}$$

These formulae can be derived using the classical perturbation approach described previously. Next, parameters $\bar{x}$, β, λ of the Weibull distribution [8] are obtained as a solution of the following system of equations:

$$E[g]=\lambda\Gamma\left(1+\frac{1}{\beta}\right)+\bar{x} \tag{6.4}$$

$$\sigma(g)=\lambda^2\left[\Gamma\left(1+\frac{2}{\beta}\right)-\Gamma^2\left(1+\frac{1}{\beta}\right)\right] \tag{6.5}$$

$$S(g)=\lambda^3\left[\Gamma\left(1+\frac{3}{\beta}\right)-3\Gamma\left(1+\frac{2}{\beta}\right)\Gamma\left(1+\frac{1}{\beta}\right)+2\Gamma^3\left(1+\frac{1}{\beta}\right)\right]\frac{1}{\sigma^2(g)} \tag{6.6}$$

where the Gamma function is defined as

$$\Gamma(x)=\begin{cases}\int_0^\infty e^{-t}t^{x-1}dt\ (for\ x>0)\\ \lim_{n\to\infty}\dfrac{n!n^{x-1}}{x(x+1)(x+2)...(x+n-1)}\ (for\ any\ x\in\Re)\end{cases} \tag{6.7}$$

Finally, the reliability index is obtained as

$$R=\exp\left[-\left(\frac{\bar{x}}{\lambda}\right)^\beta\right] \tag{6.8}$$

The application of this type of analysis to a simple two−component composite beam is shown in [179], for instance. From the computational point of view it should be underlined that the mathematical packages for symbolic computation are very useful in inversion of the Gamma function and in obtaining a direct numerical solution of the equations system presented above.

The methodology shown above and applied for homogeneous media can be used for simulation of the composite materials as well. Having proposed a general algorithm for usage of the limit function g, the corresponding various limit

functions adequate to composite materials are summarised below. The most simplified and natural formulation of the limit function is a difference between allowable and computed values of the structural state function or functions.

All limit state functions proposed and used for composites can be divided basically into three different groups. The most generalised functions, independent from the composite components type, and even from homogeneity or heterogeneity of a medium and fracture character as well as physical mechanisms of the whole process, can be classified into the first group. The functions included in the second one obey a precise definition of material fracture mechanism in terms of elastoplastic behaviour, crack formation and its propagation into the composite during the whole process. The last group is characterised by the presence of the failure function in the limit function and is therefore usually oriented to the specific groups and types of composite materials.

The most general relations are maximum stress and strain laws formulated in terms of longitudinal and transverse stresses and strain for both compression and tension as follows:

- maximum stress law:

$$\begin{aligned} g_X(X) &= \begin{cases} \sigma_{L,t} - \sigma_X \left(\sigma_X \geq 0\right) \\ \sigma_{L,c} + \sigma_X \left(\sigma_X < 0\right) \end{cases} \\ g_y(X) &= \begin{cases} \sigma_{L,t} - \sigma_y \left(\sigma_y \geq 0\right) \\ \sigma_{L,c} + \sigma_y \left(\sigma_y < 0\right) \end{cases} \\ g_y(X) &= \sigma_{LT} - \left|\sigma_S\right| \end{aligned} \tag{6.9}$$

- maximum strain law:

$$\begin{aligned} g_X(X) &= \begin{cases} \varepsilon_{L,t} - \varepsilon_X \left(\varepsilon_X \geq 0\right) \\ \varepsilon_{L,c} + \varepsilon_X \left(\varepsilon_X < 0\right) \end{cases} \\ g_y(X) &= \begin{cases} \varepsilon_{L,t} - \varepsilon_y \left(\varepsilon_y \geq 0\right) \\ \varepsilon_{L,c} + \varepsilon_y \left(\varepsilon_y < 0\right) \end{cases} \\ g_y(X) &= \varepsilon_{LT} - \left|\varepsilon_S\right| \end{aligned} \tag{6.10}$$

As can be seen, the limit functions are independent from of composite material type (fibre–reinforced or laminated) as well as from the character of its components (polymer–based, metal matrix, etc.). They originate from the mechanics of homogeneous media. However, brittle or ductile character of material damage is not taken into account in the analysis as well as the possibility of crack formation during the fatigue process. That is why more sophisticated criteria are proposed as, for instance, the one formulated as

$$g(X)=\frac{2X_1}{X_2+X_3}-\frac{X_1\sqrt{\pi X_6}}{K_{1c}}\frac{8}{\pi_2}\sqrt{\ln\sec\left(\frac{\pi}{2}\frac{2X_1}{X_2+X_3}\right)} \tag{6.11}$$

where X_1 is loading stress, X_2 yield strength, X_3 tensile stress, X_4 fracture toughness, X_5 initial crack length, X_6 crack length and calculation of K_{Ic} is presented by [91]. This limit state function allows us to combine brittle and ductile fracture type of the analysed material specimen, even in the elastoplastic range. However, as in previous formula, it is quite non-sensitive to the composite material type. Considering that, the limit state functions are combined with the failure stress or strain functions in the form of so−called quadratic polynomial failure criteria, for instance. The limit state functions proposed using such a criterion can be used for the unidirectional composite laminate in both stress and strain formulations:
− Hill−Chamis:

$$g(X)=1-\sigma_X^T F_{A,X}\sigma_X,\ g(X)=1-\varepsilon_X^T G_{A,X}\varepsilon_X \tag{6.12}$$

− Hoffman and Tsai−Wu [352]:

$$g(X)=1-\sigma_X^T F_{A,X}\sigma_X-F_{B,X}^T,\quad g(X)=1-\varepsilon_X^T G_{A,X}\varepsilon_X-G_{B,X}^T \tag{6.13}$$

Starting from the equations describing the limit function g, its probabilistic moments are calculated using the formula proposed above, but in such a case the knowledge of failure function probabilistic moments is necessary. In this context, analogous to the previous considerations, the second order perturbation method can be applied to randomise any of the reliability criteria i.e. Tsai−Hill failure criterion.

6.2 Perturbation−based Reliability for Contact Problem

To illustrate the reliability analysis implementation, the stochastic perturbation reliability analysis of the linear elastic contact analysis is carried out for a composite reinforced with spherical particles. Since the solution for the deterministic problem is known and has been worked out analytically, the probabilistic analysis is made using the package MAPLE. The reliability limit function and probabilistic moments of the contact stress computations as well as some sensitivity numerical studies are carried out by the use of this program together with the visualisation of all computed functions. This methodology can be successfully applied for randomisation of all contact problem reliability studies, where contact stresses are described by the closed form equations. Otherwise, Stochastic Finite [88,162] or Boundary Element Method [46,51,185]

computational implementations are to be made in order to get general approximate probabilistic solutions for the composite contact problems. Furthermore, the numerical approach to stochastic reliability, stochastic contact modelling and the relevant analytical computation aspects can be applied and explored in various areas of modern engineering, especially in the field of composite materials.

Let us consider the contact phenomenon between two linear elastic isotropic regions characterised by the Young moduli (e_1, e_2) and Poisson ratios (ν_1, ν_2). Let us assume that the regions have spherical shapes with radii R_1 and R_2, respectively, and that the contact is considered in a point denoted by C, as it is shown in Figure 6.1 below. The 3D view of the particle–reinforced composite plane cross–section is shown in Figure 6.2.

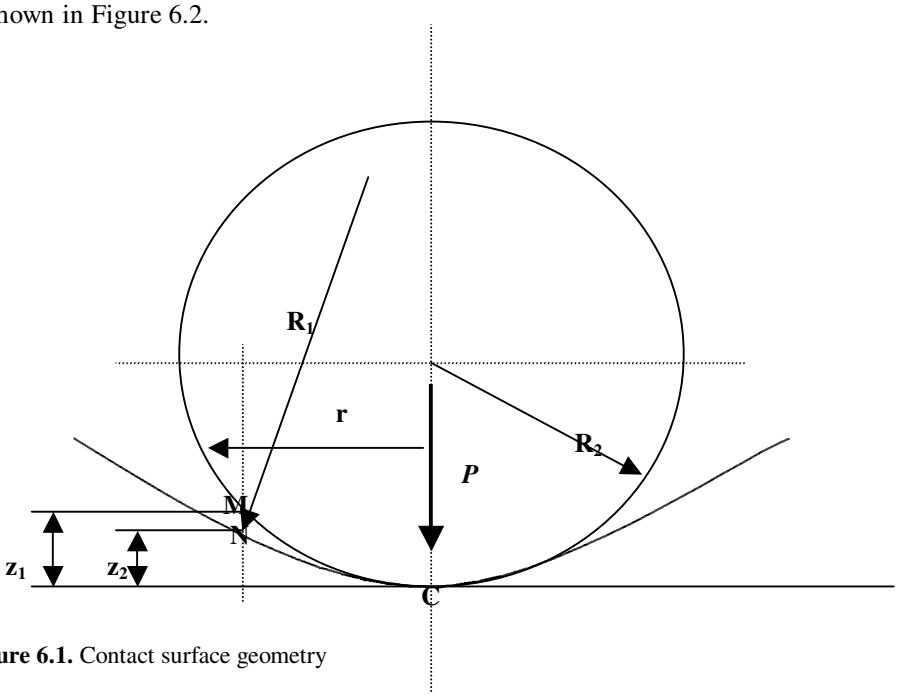

Figure 6.1. Contact surface geometry

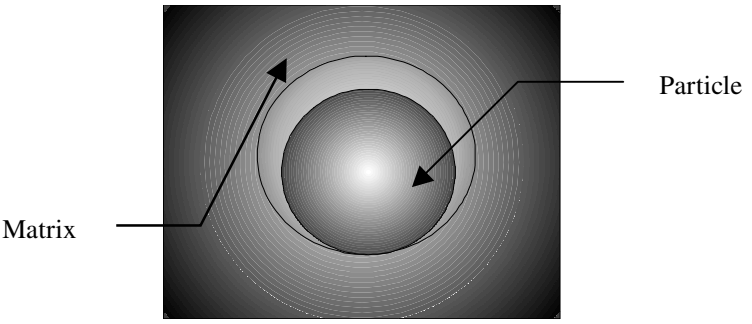

Figure 6.2. 3D view of the particle–reinforced composite plane cross–section

Let us observe that the contact problem is axisymmetric with respect to the vertical axis introduced at the centre of the spherical particle and at the bottom of this sphere (Figure 6.2). It is assumed that there is no pressure between the composite constituents and therefore the contact appears at the point C only. The distance between the points on the contacting surfaces and the plane transverse to the vertical axis of both surfaces is assumed to be small and can be described as

$$z_2 - z_1 = \frac{r^2(R_1 - R_2)}{2R_1R_2} \tag{6.14}$$

where r denotes the distance between the points M, N and the symmetry axis introduced at C. If the composite is loaded by the vertical force P acting along the vertical axis at the point C, then some local strains are induced in the neighbourhood of this point. They are a result of a contact phenomenon on a small circular surface (contact area). Assuming that the composite constituents radii R_1 and R_2 are sufficiently greater than the radius of the contact area, then the results of the Bussinesq problem of the linear elastic half−space loaded by the concentrated force can be adopted here. For this purpose let us denote by w_1 the vertical displacement induced by the local vertical strain of the point M belonging to the matrix; w_2 is the corresponding displacement of the point N in a vertical direction. Finally, assuming that the tangential plane in point C remains unmovable during a local compression, the close−up of the two points M and N can be expressed by some real η as [344]

$$\eta = \alpha - (w_1 + w_2) = \frac{r^2(R_1 - R_2)}{2R_1R_2} \tag{6.15}$$

If M and N belong to the contact area, their displacements w_i for i=1,2 can be written as

$$w_i = \frac{1-\nu_i^2}{\pi E_i} \iint q ds d\varphi \tag{6.16}$$

which follows the symmetry of the pressure intensity q and the corresponding local strains with respect to the vertical axis at the point C. Integration in this formula is carried out over the entire contact surface. Therefore

$$(k_1 + k_2) \iint q ds d\varphi = \alpha - \frac{r^2(R_1 - R_2)}{2R_1R_2} \tag{6.17}$$

Now, we are looking for such an expression for q to fulfil the above equation. It can be obtained for the pressure distribution on the contact surface represented by

the coordinates of the hemisphere with the radius a constructed on a contact surface. If q_0 is taken as the pressure at the point C, then one can show that

$$\int q ds = \frac{q_0}{a} A \tag{6.18}$$

where

$$A = \frac{\pi}{2}\left(a^2 - r^2 \sin^2 \varphi\right) \tag{6.19}$$

which gives

$$\frac{\pi(k_1 + k_2) q_0}{a} \int_0^{\frac{\pi}{2}} \left(a^2 - r^2 \sin^2 \varphi\right) d\varphi = \alpha - \frac{r^2 (R_1 - R_2)}{2R_1 R_2} \tag{6.20}$$

Finally, the parameters a and α can be determined for this problem as

$$\begin{cases} a = \sqrt[3]{\dfrac{3\pi}{4} \dfrac{P(k_1 + k_2) R_1 R_2}{R_1 - R_2}} \\ \alpha = \sqrt[3]{\dfrac{9\pi^2}{16} \dfrac{P^2 (k_1 + k_2)^2 (R_1 - R_2)}{R_1 R_2}} \end{cases} \tag{6.21}$$

which gives maximal pressure on the contact surface equal to

$$q = \frac{3P}{2\pi a^2} \tag{6.22}$$

Then, the normal stress can be defined as

$$\begin{aligned} \sigma_z &= -\int_0^a 3qr dr z^3 \left(r^2 + z^2\right)^{-5/2} \\ &= qz^3 \left| \left(r^2 + z^2\right)^{-3/2} \right|_0^a = q\left[-1 + \frac{z^3}{\left(a^2 + z^2\right)}\right] \end{aligned} \tag{6.23}$$

Let us note that the shear stresses are equal to 0, which result from the spherical symmetry of the reinforcing particle. However in the case of ellipsoidal reinforcement the shear stresses differ from 0.

The main purpose of further analysis is to determine the probabilistic characteristics of maximal contact stresses as well as contact surface geometrical parameters. Since the spherical particle surrounding the matrix is considered, let us assume that the difference R_1-R_2=ε is smaller than R_2. This parameter is treated as

input design parameter in further sensitivity analysis. The characteristics mentioned above are necessary in the final stochastic reliability computations and, considering the complexity of the equations describing reliability parameters, the stochastic second order perturbation method is proposed. The second order perturbation follows a traditional approach in this area (and the lack of convergence studies with respect to the Taylor expansion order). The third probabilistic moment method reflects the need of unsymmetric random variables modelling. Adopting the same notation as before (see Chapter 1) the skewness parameter $S(u_i)$ is calculated by

$$S(u_i) = \frac{1}{\sigma^3(u_i)} \int_{-\infty}^{+\infty} (u_i - E[u_i])^3 \, p_R(b) db \tag{6.24}$$

In further applications, the Weibull distribution is used with the probability density function defined as

$$p_R = \begin{cases} \dfrac{\beta}{\lambda}\left(\dfrac{x-\bar{x}}{\lambda}\right)^{\beta-1} \exp\left[-\left(\dfrac{x-\bar{x}}{\lambda}\right)^{\beta}\right]; x > \bar{x} \\ 0, x < \bar{x} \end{cases} \tag{6.25}$$

where β is the Weibull shape parameter, λ denotes the scale parameter and $\bar{x}$ is the location parameter, which indicates the smallest value of the random variable **x** for which the probability density function is positive. Considering this definition, the Weibull PDF is used for general mechanical applications, where many random variables must be nonnegative (Young modulus and some geometrical parameters, for instance) and especially in composite failure and fatigue modelling. Let us note that if discrete representation of a random variable $b(\mathbf{x};\theta)$ is used, then statistical estimators may be applied to approximate any order probabilistic moments of this variable.

Starting from probabilistic moments and the stochastic perturbation methodology presented above, we compute the first three probabilistic orders of the vertical stresses $E[\sigma_z(x;\omega)]$, $Var(\sigma_z(x;\omega))$ and $S(\sigma_z(x;\omega))$ as

$$E[\sigma_z] = \sigma_z^0 + \tfrac{1}{2}\sum_{i=1}^{n}\left(\frac{\partial^2 \sigma_z}{\partial b_i^2}\right)\sigma^2(b_i) \tag{6.26}$$

$$\begin{aligned}\sigma^2(\sigma_z) = \sigma_z^2 &+ \sum_{i=1}^{n}\left[\left(\frac{\partial \sigma_z}{\partial b_i}\right)^2 + \sigma_z \frac{\partial^2 \sigma_z}{\partial b_i^2}\right]\sigma^2(b_i) \\ &+ \sum_{i=1}^{n}\left(\frac{\partial \sigma_z}{\partial b_i}\frac{\partial^2 \sigma_z}{\partial b_i^2}\right) S(b_i)\sigma^3(b_i) - E^2[\sigma_z]\end{aligned} \tag{6.27}$$

and

$$S(\sigma_z)=\left\{\sigma_z^3+\frac{3}{2}\sum_{i=1}^{n}\left[2\sigma_z\left(\frac{\partial\sigma_z}{\partial b_i}\right)^2+\sigma_z^2\frac{\partial^2\sigma_z}{\partial b_i^2}\right]\sigma^2(b_i)\right.$$
$$+\left(\sum_{i=1}^{n}\left[\left(\frac{\partial\sigma_z}{\partial b_i}\right)^3+3\sigma_z\frac{\partial\sigma_z}{\partial b_i}\frac{\partial^2\sigma_z}{\partial b_i^2}\right]S(b_i)\sigma^3(b_i)\right)\frac{1}{\sigma^3(\sigma_z)} \tag{6.28}$$
$$\left.-E^3[\sigma_z]-3E[\sigma_z]\sigma^2(\sigma_z)\right\}\frac{1}{\sigma^3(\sigma_z)}$$

Having computed the first three probabilistic moments of contact stresses (expected values, standard deviations and skewness coefficients), the random field of the limit function $g(z;\omega)$ is to be proposed. Usually, it can be introduced as a difference between allowable and actual stresses $\sigma_z(z;\omega)$ induced in the composite as

$$g(z;\omega)=\sigma_{all}(\omega)-\sigma_z(z;\omega) \tag{6.29}$$

Let us underline that allowable stresses are most frequently analysed as random variables in the interior of statistically homogeneous materials, whereas actual stresses are random fields. That is why the computational analysis presented later is carried out for the specific value of the vertical coordinate z. The random variable of allowable stresses $\sigma_{all}(\omega)$ is specified by the use of the first three probabilistic moments $E[\sigma_{all}(\omega)]$, $Var(\sigma_{all}(\omega))$ and $S(\sigma_{all}(\omega))$. Then, the corresponding probabilistic characteristics of the limit function are calculated as

$$E[g]=g^0+\tfrac{1}{2}\sum_{i=1}^{n}\left(\frac{\partial^2 g}{\partial b_i^2}\right)\sigma^2(b_i) \tag{6.30}$$

$$\sigma^2(g)=\left(g^0\right)^2+\sum_{i=1}^{n}\left[\left(\frac{\partial g}{\partial b_i}\right)^2+g^0\frac{\partial^2 g}{\partial b_i^2}\right]\sigma^2(b_i) \tag{6.31}$$
$$+\sum_{i=1}^{n}\left(\frac{\partial g}{\partial b_i}\frac{\partial^2 g}{\partial b_i^2}\right)S(b_i)\sigma^3(b_i)-E^2[g]$$

as well as

$$S(g)=\left\{\left(g^0\right)^3+\frac{3}{2}\sum_{i=1}^{n}\left[2g^0\left(\frac{\partial g}{\partial b_i}\right)^2+\left(g^0\right)^2\frac{\partial^2 g}{\partial b_i^2}\right]\sigma^2(b_i)\right.$$
$$+\left(\sum_{i=1}^{n}\left[\left(\frac{\partial g}{\partial b_i}\right)^3+3g^0\frac{\partial g}{\partial b_i}\frac{\partial^2 g}{\partial b_i^2}\right]S(b_i)\sigma^3(b_i)\right)\frac{1}{\sigma^3(g)} \tag{6.32}$$
$$\left.-E^3[g]-3E[g]\sigma^2(g)\right\}\frac{1}{\sigma^3(g)}$$

Inserting the limit state function g from (6.29) into (6.30)–(6.32) and assuming that the random variable of allowable stresses and the random field of actual stresses are uncorrelated it is obtained that

$$E[g]=\sigma_{all}^0-\sigma_z^0-\tfrac{1}{2}\sum_{i=1}^{n}\left(\frac{\partial^2\sigma_z}{\partial b_i^2}\right)\sigma^2(b_i) \tag{6.33}$$

$$\sigma^2(g)=\left(\sigma_{all}^0-\sigma_z^0\right)^2+\sum_{i=1}^{n}\left[\left(\frac{\partial\sigma_z}{\partial b_i}\right)^2-\left(\sigma_{all}^0-\sigma_z^0\right)\frac{\partial^2\sigma_z}{\partial b_i^2}\right]\sigma^2(b_i)$$
$$+\sum_{i=1}^{n}\left(\frac{\partial\sigma_z}{\partial b_i}\frac{\partial^2\sigma_z}{\partial b_i^2}\right)S(b_i)\sigma^3(b_i)-E^2[\sigma_{all}-\sigma_z] \tag{6.34}$$

and, finally

$$S(g)=\left\{\left(\sigma_{all}^0-\sigma_z^0\right)^3\right.$$
$$+\frac{3}{2}\sum_{i=1}^{n}\left[2\left(\sigma_{all}^0-\sigma_z^0\right)\left(\frac{\partial\sigma_z}{\partial b_i}\right)^2+\left(\sigma_{all}^0-\sigma_z^0\right)^2\frac{\partial^2\sigma_z}{\partial b_i^2}\right]\sigma^2(b_i)$$
$$+\sum_{i=1}^{n}\left[\left(\frac{\partial g}{\partial b_i}\right)^3+3g^0\frac{\partial g}{\partial b_i}\frac{\partial^2 g}{\partial b_i^2}\right]S(b_i)\sigma^3(b_i) \tag{6.35}$$
$$\left.-E^3\left[\sigma_{all}^0-\sigma_z^0\right]-3E\left[\sigma_{all}^0-\sigma_z^0\right]\sigma^2\left(\sigma_{all}^0-\sigma_z^0\right)\right\}\frac{1}{\sigma^3\left(\sigma_{all}^0-\sigma_z^0\right)}$$

Comparing the second order second moment (SOSM) approach with the second order third moment (SOTM) approach, it is seen that the expected values are described by exactly the same equation, while standard deviations (or variances) have some extra components connected with the skewness of analysed PDF; the third order parameter of the output PDF is taken into account in the SOTM–based analysis [282].

Computational experiments are conducted by the use of the symbolic computation system MAPLE, where the stochastic second order perturbation method in W−SOTM reliability analysis of the contact problem has been implemented. The entire analysis is divided into three groups of essentially various numerical examples: (1) deterministic analysis and sensitivity study of a contact problem with respect to the vertical spatial coordinate, (2) stochastic second order perturbation based numerical modelling by randomising most of the input problem parameters and (3) stochastic numerical modelling according to the Weibull second order third moment approach.

Deterministic analysis (Figure 6.3) and the sensitivity of contact stresses in a two-component composite with spherical particles is verified with respect to the vertical spatial coordinate. The following data are adopted for the computational analysis: e_2=2.0E9, ν_1=0.3, ν_2=0.2, R_2=0.18, P=10.0E5, $\alpha=e_1/e_2$=2.0~8.0, $\beta=R_1/R_2$=1.001−1.01.

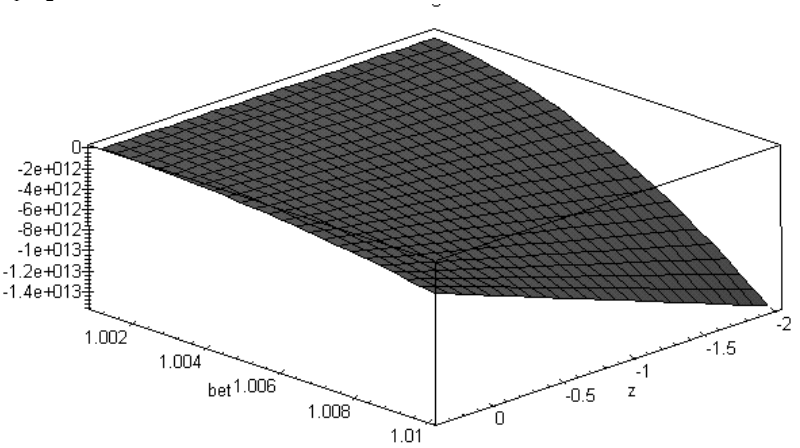

Figure 6.3. Contact stresses for the spherical particle−reinforced composite

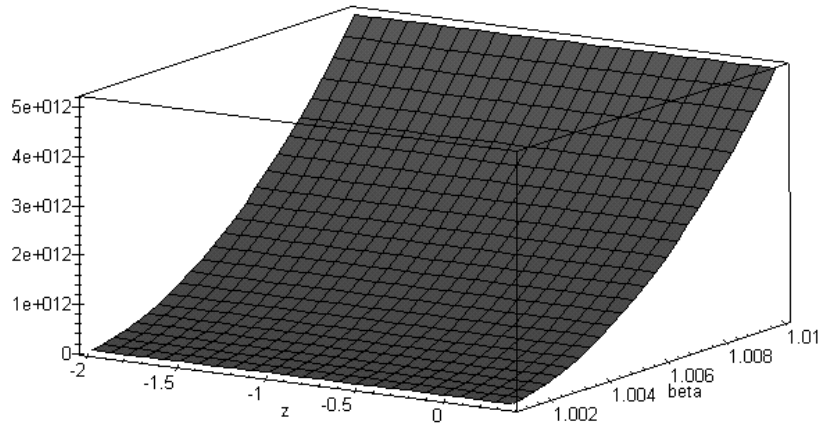

Figure 6.4. Sensitivity of contact stresses to vertical spatial coordinate '*z*'

Computational analysis of vertical contact stresses and their sensitivity gradients ($d\sigma_z/dz$) with respect to the spatial coordinate is presented in Figure 6.4. The reinforcement ratio (α) and the radii ratio (β) are marked on the vertical axes in Figures 6.3 and 6.4. The compressive contact stresses are most sensitive to the parameter β for its value tending to 0 (matrix perfectly surrounds the matrix) and for the parameter α tending to 1 (Young modulus of the reinforcing particle tends to the matrix Young modulus). One of the main benefits of the MAPLE computations, i.e. visualisation of the stress variations and their sensitivity gradients, can be studied in these figures.

All the input parameters of the analysed contact problem are treated as random variables: Young moduli and Poisson ratios of the composite components as well as their radii. Deterministically calculated vertical stresses in the contact area are compared below with expected values, standard deviations and probabilistic envelope values of the vertical contact stresses for z=0.1. The standard deviations of the variables are taken in the range of 10% of the corresponding expectations; all variables are assumed to be uncorrelated.

The computed deterministic contact stresses are shown in Figures 6.5, 6.9, 6.13 for the particle centre (z=0.09) and for the matrix (z=-0.5 and z=-2.0, respectively). The expected values of contact stresses are shown in Figures 6.6, 6.10 and 6.14 for the same points, the standard deviations are shown in Figures 6.7, 6.11 and 6.15, while the probabilistic envelopes for these stresses surfaces are presented in Figures 6.8, 6.12 and 6.16. The vertical contact stress parameters are marked on the vertical axes; horizontal axes define the reinforcement ratio of the composite (α) and the ratio between particle and the surrounding matrix radii (β). All the surfaces shown in these figures have the same character and the variability with respect to the input parameters α and β, apart from the standard deviations plots.

Analysing Figures 6.5−6.6, 6.9−6.10 and 6.13−6.14, it is seen that the expected values of contact stress surfaces are quite close to those obtained in the corresponding deterministic analyses. Essential differences are observed between Figures 6.5−6.8, 6.9−6.12 and 6.13−6.16, where probabilistic envelopes of these stresses are shown. These envelopes are determined for a particular $\mathbf{x}$ on the basis of the results presented in Figs. 6.6−6.7, 6.10−6.11 and 6.14−6.15 as

$$Env(f(x);x) = E[f(x);x] - 3sig(f(x);x) \tag{6.36}$$

Let us note that (6.36) is frequently used in the Stochastic Finite Element computations and stochastic fatigue analysis. The values of probabilistic envelope surfaces are significantly smaller than the corresponding values obtained from deterministic analysis, which means that stochastic perturbation based computational analysis more restrictive than the classical model as well as the corresponding expected values. All the surfaces combined in the probability envelope show that vertical stresses tend to 0 for the reinforcement ratio and matrix radius tending to a spherical particle radius. Comparing all deterministic and stochastic results, it is clear that the contact stresses are most sensitive to the vertical spatial coordinate.

Analysing Figures 6.5−6.8, 6.10−6.12 and 6.14−6.16 in terms of the contact stress variations with respect to the composite reinforcement ratio, it is observed that the greatest sensitivity appears for $\alpha \to 1$, which means that the greatest variations of examined probabilistic stresses are obtained for the homogeneous contact problem. Further numerical sensitivity analysis with respect to the Poisson ratio interrelations of both composite components is necessary.

The computational study on structural reliability, proposed in the theoretical considerations on structural reliability, is the main subject of the next example. The set of input data together with their probabilistic characteristics is given in Table 6.1 for the same composite contact problem as before. The Weibull probability density function (PDF) of the limit function is determined together with its up to third order probabilistic moments (cf. Table 6.1) obtained by a symbolic computational solution of the nonlinear equations system (6.30)−(6.32). The PDF of a limit function is presented in Figure 6.17 – probabilistic vertical stresses are shown on the horizontal axis, while the probability on the vertical axis.

First, it can be seen that even for a relatively small input coefficient of variation of input parameters (not greater than 0.1), the randomness level of the output function is about 18% of the relevant expected value. That is why the proposed third order approach is more accurate for the analysed contact problem. Furthermore, we observe that even for input skewnesses equal to 0, the corresponding third order probabilistic characteristics differ from 0, which reflects the differences in algebraic combinations of lower order characteristics. In further analysis it is necessary to verify the sensitivity (both in deterministic and stochastic context) of output Weibull PDF probabilistic moments with respect to all input mechanical parameters and their random characteristics. At the same time, the cross−correlation function of contact stresses can be symbolically computed using the program MAPLE.

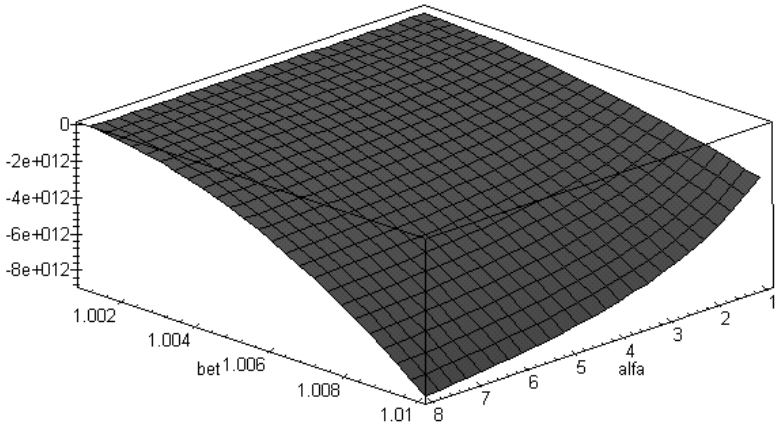

Figure 6.5. Deterministic contact stresses (z=0.018)

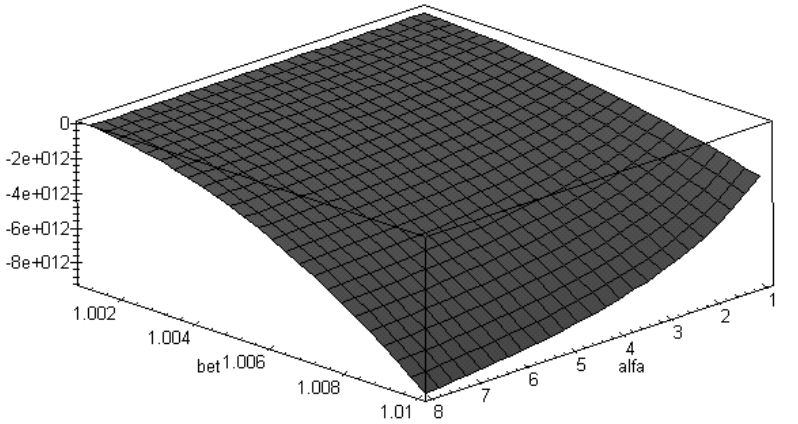

Figure 6.6. Expected values of contact stresses (z=0.018)

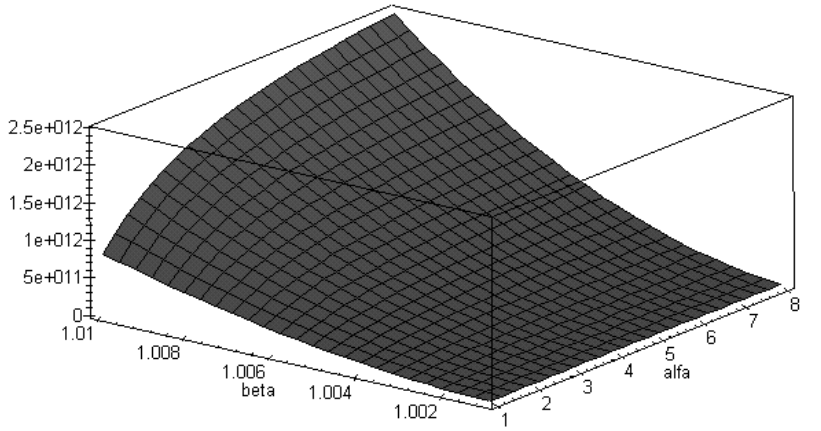

Figure 6.7. Standard deviations of contact stresses (z=0.018)

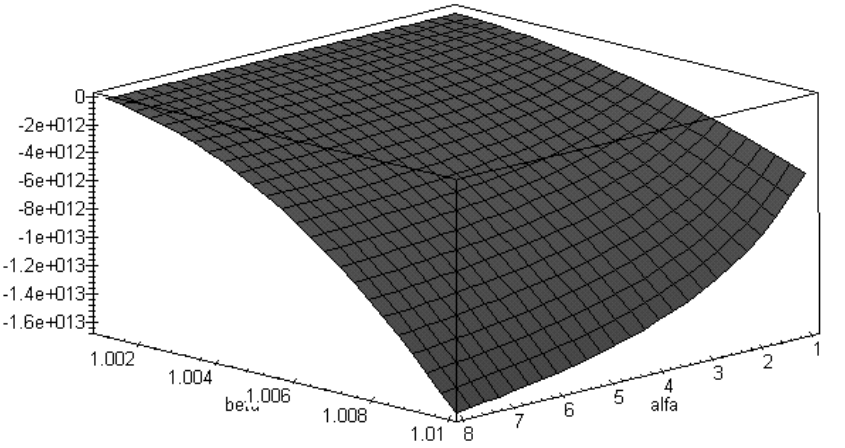

Figure 6.8. Probabilistic envelope of contact stresses (z=0.018)

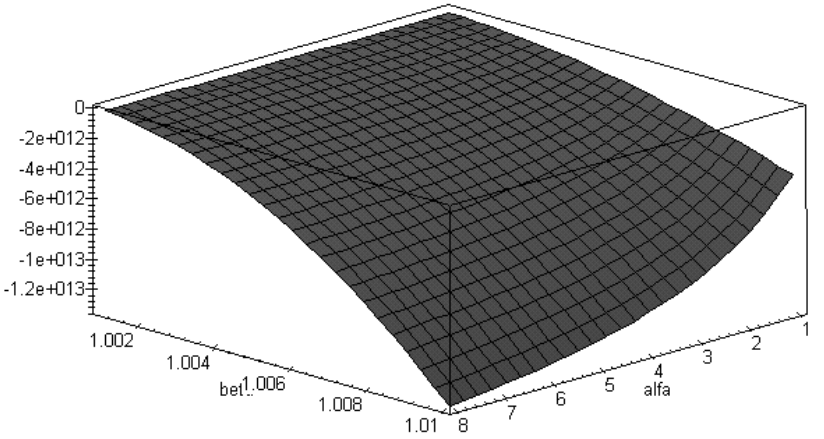

Figure 6.9. Deterministic contact stresses (z=-0.5)

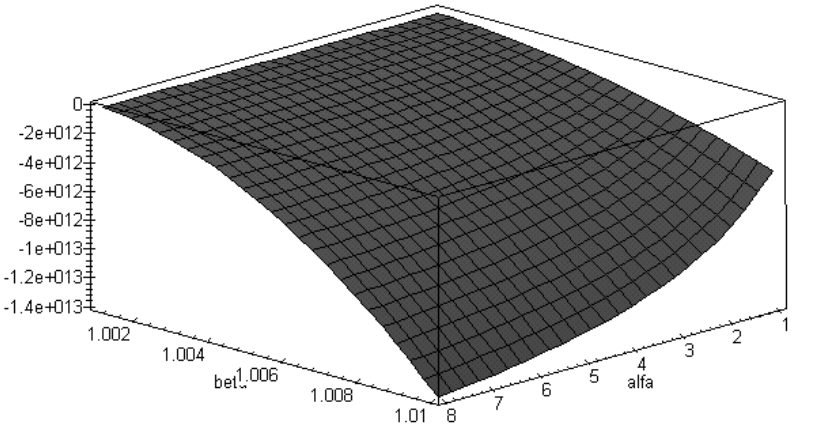

Figure 6.10. Expected values of contact stresses (z=-0.5)

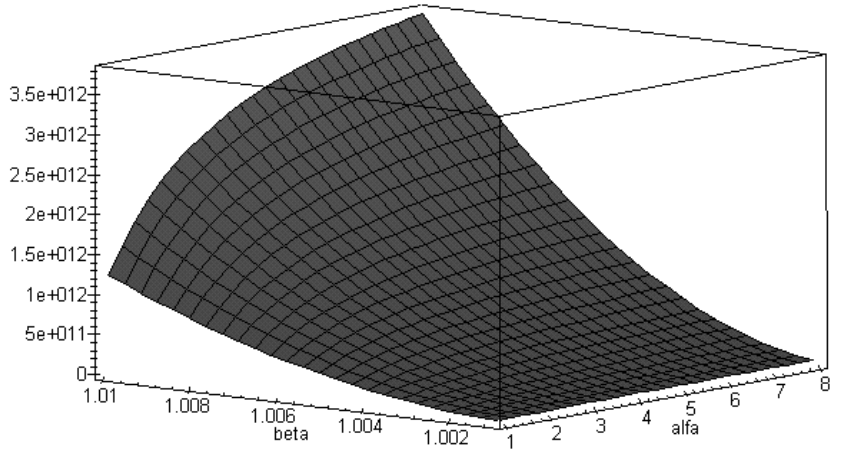

Figure 6.11. Standard deviations of contact stresses (z=-0.5)

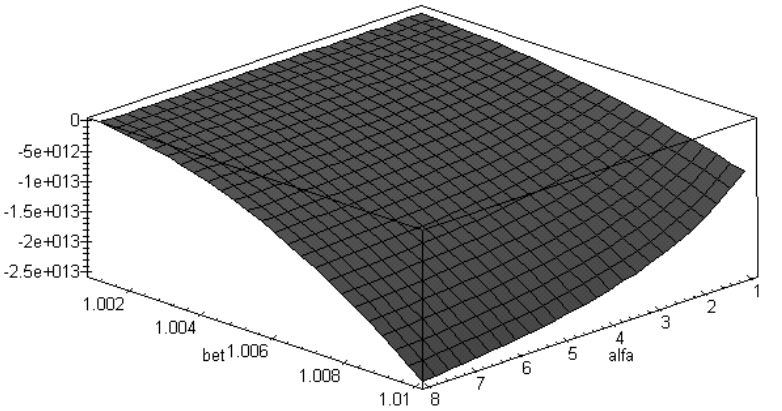

Figure 6.12. Probabilistic envelope of contact stresses (z=-0.5)

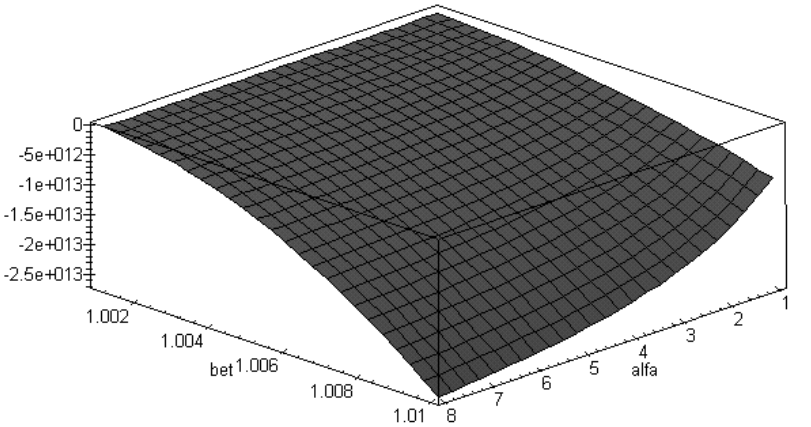

Figure 6.13. Deterministic contact stresses (z=-2.0)

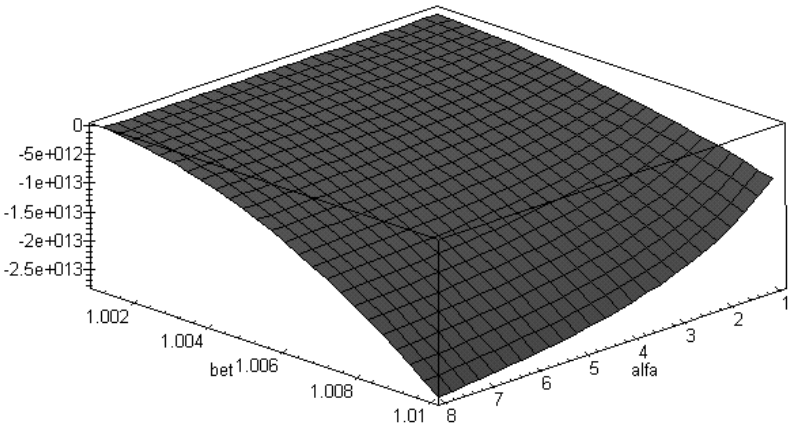

Figure 6.14. Expected values of contact stresses (z=-2.0)

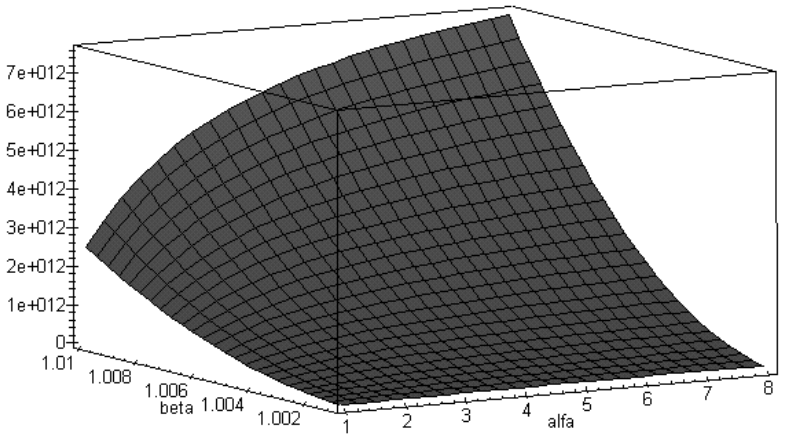

Figure 6.15. Standard deviations of contact stresses (z=-2.0)

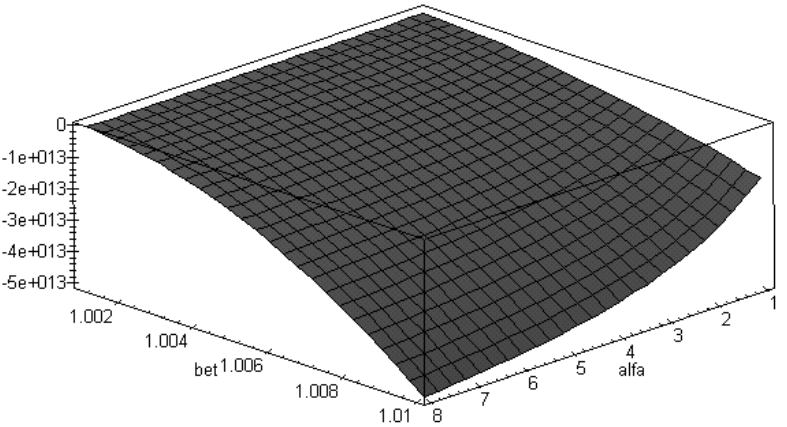

Figure 6.16. Probabilistic envelope of contact stresses (z=-2.0)

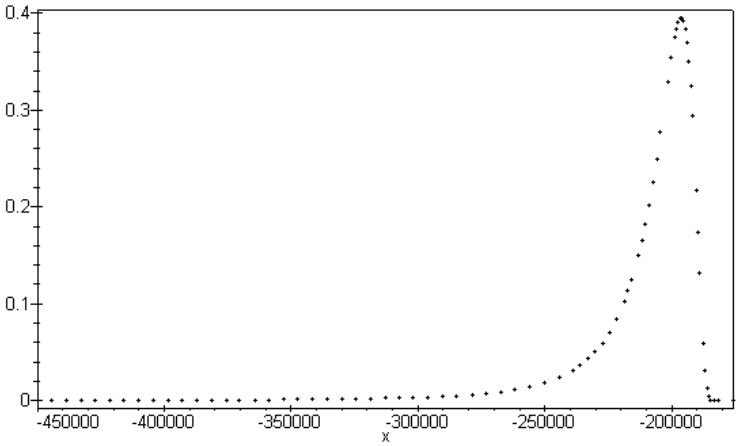

Figure 6.17. Equivalent Weibull distribution for the limit function

Table 6.1. Probabilistic input data for reliability index computations

Parameter	Value
E_2	2.0E6
ν_1	0.3
ν_2	0.2
R_2	1.8
P	5.0E2
Z	-0.018
$\sigma(e_2)$	0.2E6
$S(e_2)$	0.0
$\sigma(R_2)$	0.018
$S(R_2)$	0.0
σ_{all}	-4.0E5
α	10.0
β	1.01
$E[g]$	-211378.33
$\sigma(g)$	38213.61838 (α=0.18)
$S(g)$	5.158577

The analysis presented above reflects various sources of randomness and stochasticity in contact problems of the spherical particle reinforced composites. In comparison to the second order second probabilistic moment approach, third order probabilistic moments of both input and output parameters are analysed. It is demonstrated that even for skewnesses of the inputs equal to 0, the output third order probabilistic moments in reliability studies slightly differ from 0. It results from the main idea of the SOTM approach and from the interrelations between lower order probabilistic characteristics. Further, it is observed that deterministic values of the state functions are quite close to the computed expected values. They are considerably greater and well approximated by their probabilistic envelopes, which confirms the usefulness of these envelopes in various stochastic numerical experiments.

The most interesting extension of this study would be introducing: (1) the randomness of non-spherical contact surface (ellipsoidal one) and, next, (2) more realistic incremental Stochastic Finite or Boundary Element Method (SFEM or SBEM, respectively) of nonlinear geometry of the contacting surface. Next, the application of a computational W−SOTM reliability study in various numerical analyses of composites would be interesting, too. Neglecting relatively simple character of the deterministic contact problem, the geometrical sensitivity of the contact stress values is decisive for this analysis, both in deterministic and stochastic cases. Considering the above, one can have a conclusion that the stochastic second order perturbation analysis in a conjunction with mathematical symbolic computations is a very powerful stochastic computational tool. However, the limitations on the input randomness level typical for such an analysis must be fulfilled [208].

6.3. Stochastic Model of Degradation Process

Let us consider an engineering system $\Omega \in \Re^3$ under stochastic degradation processes (SDP) with n uncorrelated components $D(\mathbf{x};\omega;t) = D_i(\mathbf{x};\omega;t)$, i=1,..,n where $t \in [0,\infty)$. It is assumed that for every $\tau \in [0,\infty)$ the components $D_i(\mathbf{x};\omega;\tau)$ are Gaussian random variables, i.e. they are uniquely defined by their first two probabilistic moments: the expected values $E[D_i(\mathbf{x};\omega;\tau)]$ and the variances $Var(D_i(\mathbf{x};\omega;\tau))$. Due to the uncorrelation assumption, the covariance matrix for any $\tau \in [0,\infty)$ between the SDP components, it yields [176]

$$Cov\left(D_i(\mathbf{x};\omega;\tau);D_j(\mathbf{x};\omega;\tau)\right)=0;\quad i,j=1,...,n,\quad i\neq j \tag{6.37}$$

Moreover, because of the lack of respective experimental results, we assume that there are no time correlations between the SDP components

$$Cov\left(D_i\left(\mathbf{x};\omega;\tau^{(1)}\right);D_j\left(\mathbf{x};\omega;\tau^{(2)}\right)\right)=0;\quad i,j=1,...,n \tag{6.38}$$

However, in contrast to the above, the spatial correlation of particular components have non−zero values

$$Cov\left(D_i\left(\mathbf{x}^{(1)};\omega;\tau\right);D_i\left(\mathbf{x}^{(2)};\omega;\tau\right)\right)\neq 0 \tag{6.39}$$

and are computed by use of the statistical estimation methods. Let us note that, from an engineering point of view, every $D_i(\mathbf{x};\omega;t)$ for i=1,...,n represents some material (elastic characteristics or yield stress) or geometrical properties (section area, element thickness) of the system Ω under considerations.

Further, let us assume that all SDP components are statistically measured (obtained in the experimental way) in the moments $t_1,t_2,...,t_m$, for some $m \in N$. On the basis of a measured M series of these components, the basic statistical parameters are estimated by use of the following formulae:

- the expected values estimator:

$$E\left[D_i\left(\mathbf{x};\omega;t_k\right)\right]=\frac{1}{M}\sum_{i=1}^{M}D_i^{(j)}\left(\mathbf{x};\omega;t_k\right) \tag{6.40}$$

where $D_i^{(j)}(\mathbf{x};\omega;t_k)$ denotes the jth measurement of the ith SDP component in the moment t_k;

- unbiased variance estimator of the ith SDP component in the moment t_k:

$$Var\left(D_i\left(\mathbf{x};\omega;t_k\right)\right)=\frac{1}{M-1}\sum_{j=1}^{M}\left\{D_i^{(j)}\left(\mathbf{x};\omega;t_k\right)-E\left[D_i\left(\mathbf{x};\omega;t_k\right)\right]\right\}^2 \tag{6.41}$$

- standard deviation of the ith SDP component in the moment t_k:

$$\sigma\left(D_i\left(\mathbf{x};\omega;t_k\right)\right)=\sqrt{Var\left(D_i\left(\mathbf{x};\omega;t_k\right)\right)} \tag{6.42}$$

- coefficient of variation of the ith SDP component in the moment t_k:

$$\alpha\left(D_i\left(\mathbf{x};\omega;t_k\right)\right)=\sqrt{\frac{Var\left(D_i\left(\mathbf{x};\omega;t_k\right)\right)}{E^2\left[D_i\left(\mathbf{x};\omega;t_k\right)\right]}} \tag{6.43}$$

- covariance matrix estimator of the ith SDP component in the moment t_k:

$$\begin{aligned}&Cov\left(D_i\left(\mathbf{x}^{(1)};\omega;t_k\right),D_i\left(\mathbf{x}^{(2)};\omega;t_k\right)\right)\\&=\frac{1}{M-1}\sum_{j=1}^{M}\left(D_i^{(j)}\left(\mathbf{x}^{(1)};\omega;t_k\right)-E\left[D_i^{(j)}\left(\mathbf{x}^{(1)};\omega;t_k\right)\right]\right)\\&\times\left(D_i^{(j)}\left(\mathbf{x}^{(2)};\omega;t_k\right)-E\left[D_i^{(j)}\left(\mathbf{x}^{(2)};\omega;t_k\right)\right]\right)\end{aligned} \tag{6.44}$$

Next, on the basis of all statistical estimators of the SDP components $D_i\left(\mathbf{x};\omega;t\right)$ computed for the moments $t_1,t_2,...,t_m$, let us introduce the polynomial approximation of the respective probabilistic moments. This approximation is shown for the example of the expected values and the variances:

$$E\left[D_i\left(\mathbf{x};\omega;t\right)\right]=\sum_{i=1}^{p}A_p\cdot t^p\ ;\ p\le k \tag{6.45}$$

$$Var\left(D_i\left(\mathbf{x};\omega;t_k\right)\right)=\sum_{i=1}^{q}B_q\cdot t^q\ ;\ q\le k \tag{6.46}$$

where the coefficients A_p,B_q depend on estimated values of the probabilistic moments approximated in the moments $t_1,t_2,...,t_m$. Thus, on the basis of discrete values of these moments, their continuous time functions are obtained. It should be underlined that (6.45) and (6.46) enable us generally to provide an extrapolation of the expected values and variances which is the basis of the approach proposed.

Finally, let us introduce the following time continuous functions, being stochastic upper $U^{(i)}\left(x;\tau\right)$ and lower $L^{(i)}\left(x;\tau\right)$ bounds for every SDP components $D_i\left(\mathbf{x};\omega;t\right)$ in the form

$$\underset{D_i(x;\omega;\tau)}{\forall}\ \underset{\substack{U^{(i)}(x;\tau)\\ L^{(i)}(x;\tau)}}{\exists}\ P\left(D_i(x;\omega;\tau)\right)\!L^{(i)} \le D_i(x;\omega;\tau) \le U^{(i)}\Big) \cong 1 \tag{6.47}$$

To obtain these bounds for some $\tau \in [0,\infty)$, the well−known following bounds for Gaussian variables are used

$$U^{(i)}(x;\tau) = E[D_i(x;\omega;\tau)] + 3\sqrt{Var(D_i(x;\omega;\tau))} \tag{6.48}$$

$$L^{(i)}(x;\tau) = E[D_i(x;\omega;\tau)] - 3\sqrt{Var(D_i(x;\omega;\tau))} \tag{6.49}$$

It should be noted that the interval $\left[L^{(i)}(x;\tau), U^{(i)}(x;\tau)\right]$ can be contracted by decreasing the coefficient multiplied by the standard deviations of $D_i(\mathbf{x};\omega;\tau)$ in (6.48) and (6.49). However the probability value specified in (6.47) will decrease respectively as a result.

As was stated above, the main purpose of our analysis is to make a prognosis of the stochastic reliability and failure time and/or to compute the safety interval for the respective design parameters of the engineering system Ω considered. Taking this into account, there are two kinds of boundary conditions: the *1*st kind, of stress (load capacity conditions) and the *2*nd kind, of displacement type (service conditions). Finally, the following inequalities are to be verified simultaneously to find out the time prognosis of the engineering structural safety:

$$\begin{cases} U[\sigma_{\max}(x;\omega;t)] \le L[\sigma_{all}(x;\omega;t)] \\ U[\mathbf{u}_{\max}(x;\omega;t)] \le L[\mathbf{u}_{all}(x;\omega;t)] \end{cases} \tag{6.50}$$

where $u_{\max}$ and $\sigma_{\max}$ are maximal values of displacements and stresses, while quantities indexed with 'all' are allowable values. Solving the set of inequalities (6.50) iteratively with given time increment Δt, the failure time t_f can be found as such a value, for which one of these inequalities does not hold as the first one.

It should be noted that these inequalities are based on the comparison of the upper bounds of the maximal stresses and displacement stochastic processes and the lower bounds of the allowable stresses and displacement stochastic processes. Moreover, the lower bounds from the right sides of the system (6.50) can be derived on the basis of the given SDP components $D_i(\mathbf{x};\omega;\tau)$ or given explicitly as deterministic values being an effect of simplified engineering calculations. On the other hand, the probabilistic moments of the maximal stresses and displacements can be evaluated by the collocation of the simulation technique or stochastic perturbation method with analytical solutions of the given problem or various numerical methods. Finally, let us note that the methodology presented can be efficiently used in conjunction with stochastic fatigue and fracture theories [89,377] and can extend the existing probabilistic strength models [142].